



1 **Effectiveness and limitations of parameter tuning in**  
2 **reducing biases of top-of-atmosphere radiation and clouds**  
3 **in MIROC version 5**

4

5 **Tomoo Ogura<sup>1</sup>, Hideo Shiogama<sup>1</sup>, Masahiro Watanabe<sup>2</sup>, Masakazu Yoshimori<sup>3</sup>,**  
6 **Tokuta Yokohata<sup>1</sup>, James D. Annan<sup>4</sup>, Julia C. Hargreaves<sup>4</sup>, Naoto Ushigami<sup>5</sup>,**  
7 **Kazuya Hirota<sup>2</sup>, and Yu Someya<sup>2</sup>**

8 [1] National Institute for Environmental Studies, Tsukuba, Ibaraki, Japan

9 [2] Atmosphere and Ocean Research Institute, University of Tokyo, Kashiwa, Chiba, Japan

10 [3] Faculty of Environmental Earth Science, Global Institution for Collaborative Research and  
11 Education, and Arctic Research Center, Hokkaido University, Sapporo, Hokkaido, Japan

12 [4] BlueSkiesResearch.org.uk, Settle, North Yorkshire, United Kingdom

13 [5] University of Tsukuba, Tsukuba, Ibaraki, Japan

14 Correspondence to: T. Ogura ([ogura@nies.go.jp](mailto:ogura@nies.go.jp))

15

16 **Abstract**

17 This study discusses how much of the biases in top-of-atmosphere (TOA) radiation and  
18 clouds can be removed by parameter tuning in the present-day simulation of a climate model  
19 in the Coupled Model Inter-comparison Project phase 5 (CMIP5) generation. We used a low-  
20 resolution version of the Model for Interdisciplinary Research on Climate version 5  
21 (MIROC5) Atmosphere-Ocean General Circulation Model (AOGCM) and compared the  
22 output of a perturbed parameter ensemble (PPE) experiment in the pre-industrial control  
23 setting with satellite observation data. The model biases and the parametric uncertainty of the  
24 biases are evaluated with respect to TOA radiation and clouds. We used the output of the PPE  
25 experiment without flux adjustment, which is consistent with the experimental design of the  
26 CMIP5. The results indicate that removing or changing the sign of the biases by parameter  
27 tuning alone is difficult. Especially, the cooling bias of the shortwave cloud radiative effect in  
28 low latitudes could not be removed, neither in the zonal mean nor at each latitude–longitude



1 grid point. The bias was related to the overestimation of both cloud amount and cloud optical  
2 thickness, which could not be removed by the parameter tuning either. However, they could  
3 be alleviated by tuning parameters such as the maximum cumulus updraft velocity at the  
4 cloud base. On the other hand, the bias of the shortwave cloud radiative effect in the Arctic  
5 was sensitive to parameter tuning. It could be removed by tuning such parameters as albedo of  
6 ice and snow both in the zonal mean and at each grid point. The obtained results illustrate the  
7 benefit of PPE experiments which provide useful information regarding effectiveness and  
8 limitations of parameter tuning.

9

## 10 **1 Introduction**

11 The climate models used in Coupled Model Inter-comparison Project phase 5 (CMIP5) still  
12 exhibit significant biases in simulating present-day top-of-atmosphere (TOA) radiation, as in  
13 CMIP3 (Flato et al. 2013). The biases are especially large in the component of the shortwave  
14 cloud radiative effect (SCRE), namely the difference in shortwave radiation between all-sky  
15 and clear-sky values. The SCRE represents the radiative effect of clouds, which cool the  
16 climate system by reflecting shortwave radiation. Compared with satellite observations,  
17 however, the cooling effect of the SCRE tends to be overestimated over low-latitude oceans  
18 and underestimated over the Southern Ocean, suggesting that the models still have difficulties  
19 in simulating clouds in these regions (Nam et al. 2012, Bodas-Salcedo et al. 2014). Previous  
20 studies suggest that such biases in radiation and clouds might affect the simulated climate in  
21 remote regions or distort the cloud feedback in future projections (Trenberth and Fasullo 2010,  
22 Ceppi et al. 2012). Therefore, alleviating the biases by developing climate models is  
23 important.

24 There are two factors, which might contribute to the biases in climate simulated by the  
25 models: (a) inappropriate model structures, namely, equations representing the physical  
26 processes or spatial resolution of the model; and (b) inappropriate parameter values, which are  
27 specified in the equations. We therefore attempt to alleviate the biases by modifying the  
28 factors (a) and (b) within the plausible range during the model development process.

29 How much of the existing biases can be explained by the second factor (b)? In other words,  
30 how much of the biases can be removed by modifying only specified parameter values  
31 (parameter tuning)? This issue is important when discussing the model development strategy  
32 because it helps to decide which factor, (a) or (b), should be given a priority to efficiently



1 reduce the biases. If all biases can be explained by factor (b), the priority for parameter tuning  
2 would be high. In this case, removing the biases is relatively simple because parameter tuning  
3 is generally much easier than modifying the model structures. On the contrary, if most of the  
4 biases cannot be explained by factor (b), modifying model structures should be given a high  
5 priority.

6 A Perturbed Parameter Ensemble (PPE) experiment with a climate model is useful when  
7 discussing the above issue. In the PPE experiment, we can create different versions of a  
8 climate model in a systematic and comprehensive way by modifying the specified parameter  
9 values in the model within a plausible range (Murphy et al. 2004). If we evaluate the biases  
10 by comparing present-day climate with observation data in each version of the PPE models,  
11 we should be able to evaluate parametric uncertainty, namely, the inter-model difference of  
12 the biases due to parameter settings. This inter-model difference would also provide a  
13 measure regarding how much of the biases can be removed by parameter tuning only.

14 The benefit of PPE experiments, as discussed above, has been illustrated in previous studies.  
15 For example, Zhang et al. (2012) conducted a PPE experiment with an Atmosphere General  
16 Circulation Model (AGCM) and evaluated the performance of cloud simulations compared  
17 with satellite observations over various tropical regions. The results indicate that the model  
18 performance in simulating clouds is sensitive to parameter tuning. Yokohata et al. (2012)  
19 focused on different PPE experiments conducted with an Atmosphere-Ocean GCM  
20 (AOGCM), two Atmosphere-Slab ocean GCMs (ASGCMs), and an AGCM and evaluated the  
21 model performance in simulating the cloud radiative effect at TOA compared with  
22 observations. They found that the sensitivity of the model biases to parameter tuning varies  
23 widely among different regions. In the PPEs analyzed in the study, however, the sea surface  
24 temperature (SST) bias was suppressed by applying flux adjustment at the sea surface in both  
25 AOGCM and ASGCM.

26 In the present study, we attempt to better understand the parametric uncertainty of TOA  
27 radiation and cloud biases by using the PPE output of an AOGCM without flux adjustment.  
28 There is an advantage in using the AOGCM without flux adjustment because climate  
29 projections in the CMIP5 Multi-Model Ensemble (MME) are conducted with AOGCMs  
30 without flux adjustment and the biases of such AOGCMs are therefore directly relevant for  
31 future projections using CMIP5 (Flato et al. 2013). If we suppress the SST biases in the  
32 AOGCMs by applying flux adjustment, the TOA radiation and cloud biases in which we are



1 interested might be obscured. In addition, the parametric uncertainty of the biases might be  
2 overestimated if we apply flux adjustment because it allows us to include AOGCMs with  
3 large radiative imbalance at the TOA as valid samples in the PPE, while such models are not  
4 used for future projections in the CMIP5 MME.

5 When evaluating biases in the simulated clouds, we use output of the Cloud Feedback Model  
6 Inter-comparison Project (CFMIP) Observation Simulator Package (COSP), which is  
7 incorporated in the AOGCM. The COSP is diagnostic software that processes the GCM  
8 outputs, such as the cloud amount, and simulates the signals that would be retrieved by  
9 satellites if the model-generated clouds existed in the real world (Bodas-Salcedo et al. 2011).  
10 It increases the chances that the difference between the model output and observation reflects  
11 real biases in the model simulation rather than observational limitations. Therefore, COSP has  
12 been widely used in previous studies, which evaluate clouds simulated by the CMIP5 MME.  
13 The studies indicate that the optical thickness of the simulated clouds tends to be  
14 overestimated compared with the observation, as in the CMIP3 (Klein et al. 2013, Nam et al.  
15 2012, Zhang et al. 2005). In the present study, we evaluate the parametric uncertainty of this  
16 "too thick (bright) bias" by analyzing the COSP output of the PPE experiment and discuss  
17 how much of the bias can be removed by parameter tuning only.

18 Section 2 describes the AOGCM, design of the PPE experiment, and observation data used  
19 for the evaluation. In Section 3, we identify the biases in the TOA radiation and clouds and  
20 discuss the parametric uncertainty of the biases. We then focus on clouds over low-latitude  
21 oceans to examine if the "too thick bias" can be controlled by parameter tuning. In addition,  
22 we discuss which tuning parameters are effective in controlling the TOA cloud radiative  
23 effect. Finally, we summarize the conclusions and discuss their implications for the  
24 effectiveness and limitations of parameter tuning in Section 4.

25

## 26 **2 Models and Methods**

### 27 **2.1 Design of the Perturbed Parameter Ensemble**

28 We compared the output of the PPE experiment using the AOGCM in the pre-industrial  
29 control setting with the observation to evaluate the model biases. We used the Model for  
30 Inter-disciplinary Research on Climate version 5 (MIROC5) AOGCM. The atmospheric  
31 component has a horizontal resolution of T42 (~2.8°) with 40 vertical levels. The ocean



1 component is COCO4.5 with a horizontal resolution of  $\sim 1^\circ$  and 49 vertical levels in addition  
2 to a bottom boundary layer. The model is the low-resolution version of the MIROC5  
3 AOGCM, which is used in CMIP5 with a higher resolution of T85 ( $\sim 1.4^\circ$ ) in the atmosphere  
4 (Watanabe et al. 2010). We confirmed that the low-resolution version ran stably and did not  
5 suffer from significant climate drift in the pre-industrial control experiment without flux  
6 adjustment when the standard setting of the tuning parameters was specified. The model could  
7 also reproduce the characteristic biases of the TOA radiation and clouds of the T85 version  
8 used in CMIP5.

9 We should note that perturbing specified values of tuning parameters might increase the net  
10 radiation imbalance at TOA when conducting PPE with an AOGCM in the pre-industrial  
11 control setting, which leads to a gradual change in climate different from the initial state  
12 (climate drift). Such a change would make the definition of the control climate difficult. In  
13 addition, the simulated climate might not be a valid example of pre-industrial control  
14 simulations. Applying flux adjustment at the sea surface would help to suppress the climate  
15 drift by reducing the SST biases. However, it might also cover up the biases in the TOA  
16 radiation and clouds, which are sensitive to the SST. What we need here is both stable climate  
17 and SST biases, as indicated in the CMIP5 pre-industrial control experiments. Therefore, we  
18 used the output of the PPE experiment conducted in Shiogama et al. (2012), following the  
19 Suppressed Imbalance Sampling (SIS) method, in the present study. The SIS is a method to  
20 subsample members of the PPE with a small imbalance in the TOA radiation and thus with  
21 small climate drift. This enables us to study stable climates of the PPE without applying flux  
22 adjustment. Other methods analogous to the SIS have been discussed in Jackson et al. (2012)  
23 and Yamazaki et al. (2013).

24 The details of the SIS method are described in Shiogama et al. (2012). For reference, we also  
25 present the summary in the following. First, we select ten tuning parameters, which are  
26 considered important to the radiative forcing of CO<sub>2</sub> doubling, climate feedback, and climate  
27 sensitivity (Table 1). The selection is based on the results of sensitivity experiments using the  
28 atmospheric component of MIROC5, which shows that perturbing the ten parameters has  
29 large impact on the radiative forcing and climate feedback compared to other tuning  
30 parameters. The selected ten parameters are related to cumulus convection, cloud, turbulence,  
31 aerosol, and land surface processes. The maximum and minimum values of the parameters are  
32 determined by expert judgement so that the parameters are within the plausible range, namely,



1 they are consistent with the observation and current understanding of the climate system.  
2 Values of the ten parameters are then selected from the maximum to minimum ranges and  
3 randomly paired to produce 5000 samples of ten dimensional vectors, following Latin  
4 Hypercube Sampling. Each vector corresponds to a set of input values for the ten tuning  
5 parameters. We further select 56 members from the 5000 samples so that the TOA radiative  
6 imbalance of the selected members is close to that of the standard model. The TOA radiative  
7 imbalance of the 5000 samples is estimated using the output of a PPE separately conducted  
8 using the atmospheric component of MIROC5. The number of subsampled members, namely  
9 56, is determined by the computational resources available. Note that the number increased  
10 from 35 in the previous study by Shiogama et al. (2012). Finally, we create 56 members of the  
11 MIROC5 AOGCM by specifying different members of the ten dimensional vectors for the  
12 model as input values for the tuning parameters.

13 We ran the 56 members of the model for 30 years with the pre-industrial control setting and  
14 confirmed that the changes in the simulated surface air temperature from the initial state  
15 (climate drift) were small. This was expected because the TOA radiative imbalance is close to  
16 that of the standard model. Years 1–10 of the simulation were considered to be a spin-up  
17 period during which the simulated climate adjusted to the modified tuning parameters. The  
18 output from years 11–30 was averaged to make a climatology. The model biases were defined  
19 as the difference of the climatology from observation data.

20 The observation data used for the model evaluation originate in the period of 1983-2010  
21 (Table 2). Therefore, the model output from the historical simulation of the same period is  
22 appropriate for comparison with the observation. However, conducting the historical  
23 simulation requires an extension for more than 150 years after the pre-industrial control  
24 simulation of 30 years. This means more than 6-fold increase in computational cost, which we  
25 are not able to cover. Therefore, we decided to use the pre-industrial control simulation as a  
26 surrogate for the historical simulation, assuming that the former reproduces the biases in the  
27 latter, regarding TOA radiation and clouds. This assumption is supported by other simulation  
28 results. For example, we compared biases in the historical simulation with those in the pre-  
29 industrial control simulation using MIROC5 with the horizontal resolution of T85 (~1.4°). We  
30 confirmed that the TOA radiation and cloud biases in the two simulations were similar to each  
31 other (not shown).



## 1 2.2 Observation data

2 Table 2 summarizes the observation data which are compared with the model output. They  
3 all are monthly mean data. We defined the model biases referring to multiple observations,  
4 namely three for TOA radiation and two for the cloud amount; therefore, the observation  
5 uncertainty can be taken into account. The biases are considered robust if they are commonly  
6 seen with respect to multiple observations. The observation data for TOA radiation are  
7 derived from CERES-EBAF (Loeb et al. 2009), ERBE-S9 (Barkstrom 1984), and ISCCP-FD  
8 (Zhang et al. 2004). The data for the cloud amount are from GCM simulator-oriented ISCCP  
9 cloud product (Pincus et al. 2012, Rossow et al. 1996) and CALIPSO-GOCCP (Chepfer et al.  
10 2010). The cloud amount data of the ISCCP are custom-built daytime-only monthly averages,  
11 which are available from the CFMIP-OBS website  
12 (<http://climserv.ipsl.polytechnique.fr/cfmip-obs>). We first referred to the observation data to  
13 calculate the monthly climatology for the period in Table 2. We then interpolated the data  
14 linearly to the horizontal resolution of T42 and used them to calculate the difference from the  
15 model output.

16 When evaluating biases of clouds simulated by MIROC5 AOGCM, we used the output of  
17 the satellite simulation software COSP (version 1.2.2), which was implemented in the model;  
18 COSP includes software simulating satellite observations of ISCCP (Klein and Jakob 1999;  
19 Webb et al. 2001) and CALIOP lidar (Chepfer et al. 2008). We compared the cloud amount  
20 identified by the ISCCP simulator with the GCM simulator-oriented ISCCP cloud product and  
21 the one determined with the CALIOP lidar simulator with the CALIPSO-GOCCP data. We  
22 confirmed that the ISCCP simulator was implemented properly in the MIROC5 AOGCM  
23 following Zelinka et al. (2012), which means, we calculated the total sum of the cloud amount  
24 from the ISCCP simulator for all cloud top pressure and optical thickness bins and confirmed  
25 that the sum is consistent with the "native" cloud amount identified in MIROC5 AOGCM.  
26 Note that optically thin clouds with  $\tau < 0.3$  are not included in this comparison because the  
27 available "native" cloud amount does not include such clouds.

28

## 29 3 Parametric uncertainty of the TOA radiation bias

30 First, we present the outline of the TOA radiation bias of the MIROC5-PPE by discussing  
31 the global annual mean values in Figure 1. The biases in the net radiation are small (Figure  
32 1a), which means that the values of all PPE members are within the range of the three



1 observations and near the zero net radiation with no imbalance, indicated by the dashed line.  
2 This was expected because we selected these members when designing the PPE following the  
3 SIS method. If we focus on the components of the TOA radiation, however, we notice larger  
4 biases compared with the net radiation (Figures 1b,c). The largest biases appear in the SCRE;  
5 the biases range from  $-11.8 \text{ W/m}^2$  to  $-5.8 \text{ W/m}^2$ . All PPE members are more than  $3.0 \text{ W/m}^2$   
6 smaller than either one of the three observations. Therefore, parameter tuning enables us to  
7 reduce the bias from  $-11.8 \text{ W/m}^2$  to  $-5.8 \text{ W/m}^2$  by as much as 50 percent; however, we cannot  
8 totally remove it or change its sign. The shortwave clear-sky component (SWclr) also exhibits  
9 large biases in which all PPE members are larger than either one of the three observations.  
10 Therefore, we cannot change the sign of the bias by parameter tuning only.

11 Next, we discuss the characteristics of the radiation bias on a smaller spatial scale, as shown  
12 by the zonal annual mean in Figure 2. We especially focus on the cloud radiative effect,  
13 which illustrates the biases related to clouds. The negative SCRE biases, as observed in the  
14 global mean (Figure 1c), are mostly attributable to the biases in low latitudes (Figure 2a). In  
15 those latitudes, all PPE members are outside the range of the three observations. Therefore,  
16 the bias cannot be eliminated or change the sign by parameter tuning, although it can be  
17 reduced by ~30 percent. In the Arctic, on the other hand, the inter-model difference among  
18 the PPE members tends to be larger compared with other latitudes; hence, the observations lie  
19 within the PPE spread. Here, the SCRE bias can be eliminated or change the sign by  
20 parameter tuning. The biases of the Longwave Cloud Radiative Effect (LCRE) appears to be  
21 small in most latitudes (Figure 2b). At least one of the PPE members is within the range of the  
22 three observations.

23 The characteristics on an even smaller spatial scale are illustrated by the geographical  
24 distribution of the annual mean cloud radiative effect biases in Figures 3a and b. We used  
25 CERES–EBAF as the observation because it measures the radiative fluxes more directly than  
26 the ISCCP–FD and it also has various advantages over the ERBE–S9 such as scene  
27 identification (Wielicki et al. 1996, Loeb et al. 2009). We confirmed that similar results were  
28 obtained when using ISCCP–FD or ERBE–S9 (not shown).

29 The negative SCRE bias in the low latitudes, as observed in the zonal mean plot (Figure 2a),  
30 appears pronounced over the oceans, exceeding  $-40 \text{ W/m}^2$  in large areas (Figure 3a). We also  
31 notice positive biases in middle to high latitudes over the Southern Ocean, northwestern part  
32 of Eurasia, and northeastern part of North America. They exceed  $5 \text{ W/m}^2$  in some places. On



1 the other hand, if we measure the parametric uncertainty of the SCRE bias using the standard  
2 deviation among the PPE members, we notice that the uncertainty does not exceed  $4 \text{ W/m}^2$   
3 in most areas (Figure 3c). Therefore, removing or changing the sign of the SCRE bias at each  
4 grid point by parameter tuning only is difficult. This can be confirmed by the fractions of the  
5 PPE members, which have positive biases (Figure 3e). The fraction is 0 (blue) or 1 (orange) in  
6 most areas on the globe, namely, all PPE members have the same SCRE bias sign. Parameter  
7 tuning plays only a limited role in reducing the SCRE bias; especially, the sign of the bias  
8 cannot be changed. An exception is the Arctic. Here, the SCRE bias is smaller than  $5 \text{ W/m}^2$   
9 and the standard deviation of the bias ranges from  $6\text{--}8 \text{ W/m}^2$  (Figures 3a,c). Therefore, the  
10 biases of the PPE members can be either positive or negative, which is indicated by the green  
11 colour in Figure 3e. Here, we can change the sign of the SCRE bias by parameter tuning.

12 The LCRE bias is smaller than the SCRE bias (Figures 3a,b). It is smaller than  $20 \text{ W/m}^2$  in  
13 most areas. However, the standard deviation of the LCRE bias is even smaller (Figure 3d),  
14 less than  $5 \text{ W/m}^2$ , except for the limited area in the tropics. Therefore, we cannot change the  
15 sign of the LCRE bias by parameter tuning. This is illustrated by the fractions of the PPE  
16 members, which have positive biases (Figure 3f). They are 0 (blue) or 1 (orange) in most  
17 places including the Arctic.

18

#### 19 **4 Parametric uncertainty of the cloud bias**

20 To better understand the origin of the cloud radiative effect bias, we examine the  
21 geographical distribution of the cloud amount bias in Figure 4. In the following, we present  
22 results for the boreal summer season when the cloud amount bias is most pronounced in the  
23 Hawaiian Trade Cumulus Region, which we discuss later in this section. The cloud amount is  
24 overestimated over the Pacific and Atlantic in low latitudes (Figures 4a,b), which contributes  
25 to the negative SCRE bias, as shown in Figure 3a. The overestimation is a robust feature; it  
26 exists with respect to both ISCCP and CALIPSO observations. In addition, all members of the  
27 PPE have positive biases in those regions (Figures 4c,d). Therefore, the biases cannot be  
28 removed by parameter tuning. We should note here that the multi-model mean ISCCP cloud  
29 amount ( $\tau > 1.3$ ) from the CFMIP1 and CFMIP2 ensembles does not show such positive  
30 bias in low latitudes (Klein et al. 2013). Therefore, the bias might be a problem specific to the  
31 MIROC5 AOGCM.



1 The cloud amount bias can be decomposed into the contributions from different cloud top  
2 pressure and optical thickness bins, as illustrated for the Hawaiian Trade Cumulus Regions  
3 (15-35N, 160E-140W) in Figure 5. The region of focus is indicated by the black square in  
4 Figure 4b.

5 The MIROC5-PPE tends to overestimate optically thick clouds ( $\tau > 3.6$ ) and underestimate  
6 optically thin clouds ( $\tau < 3.6$ ) compared with the ISCCP observation (Figures 5a,b,c). The  
7 contribution of the former outweighs that of the latter, which leads to the overestimation of  
8 the cloud amount. The overestimation is especially large in low-top clouds ( $p_c > 680$ ). The  
9 clouds of the MIROC5-PPE are biased towards optically thick clouds compared with the  
10 observation, which also contributes to the negative SCRE bias.

11 We further examined the signs of the cloud biases for each bin of the cloud top pressure and  
12 optical thickness categories. The fraction of the positive biases within the PPE members is 0  
13 (blue) or 1 (orange) in 36 out of 42 bins (Figure 5d); all PPE members have the same cloud  
14 bias sign in most (85%) of the cloud top pressure and optical thickness bins. Therefore,  
15 removing the "too thick bias" by parameter tuning only is considered difficult in this model.

16 The overestimation of both the cloud amount and optical thickness ("too thick bias")  
17 contributes to the negative SCRE bias. To illustrate the importance of the "too thick bias" for  
18 the SCRE bias, we plot the relationship between the SCRE and low-top cloud amount in  
19 Figure 6. Note that we selected data of low-top clouds, which are not overlapped by middle-  
20 top or high-top clouds in the figure; hence, the SCRE is not affected by clouds other than the  
21 low-top clouds, which prevail in the Hawaiian Trade Cumulus Region. The figure shows that  
22 SCRE negatively increases as the low-top cloud amount increases in both the observation and  
23 MIROC5-PPE. However, the MIROC5-PPE shows a negatively larger SCRE compared with  
24 the observation. It is larger by  $\sim 30 \text{ W/m}^2$ , even if the models have the same cloud amount as  
25 the observation, which indicates that the optical thickness of low-top clouds is overestimated  
26 in the MIROC5-PPE. The above-mentioned characteristics are common to all PPE members  
27 and the observation is outside the range of the PPE. This again indicates that we cannot  
28 remove the "too thick bias" by parameter tuning only.

29



## 1 5 Characteristics of different tuning parameters

2 The results presented so far illustrate the difficulties in removing the TOA radiation and  
3 cloud biases by parameter tuning. At the same time, however, we also learned that parameter  
4 tuning enables us to control the model biases to some extent, demonstrating its benefit for  
5 model development. For example, the global mean SCRE bias can be reduced by as much as  
6 50% by tuning only (Figure 1c). To obtain the desired effects by parameter tuning, we need to  
7 understand the characteristics of different tuning parameters. Therefore, in the following, we  
8 briefly describe the regions in which the tuning parameters in Table 1 control the model  
9 biases, focusing on the CRE.

10 We calculated the regression coefficients of the CRE on different tuning parameters for each  
11 latitude–longitude grid point, referring to the 56 members of the PPE, and plotted the  
12 geographical distribution of the coefficients in Figures 7 and 8. In addition, we calculated the  
13 regression of the ISCCP cloud properties (cloud amount, cloud optical thickness, and cloud  
14 top pressure) on the tuning parameters. The results are shown in the Appendix Figures A1, A2,  
15 and A3. Note that the tuning parameters were normalized to the range of 0.0 to 1.0; thus, the  
16 coefficients indicate the responses of the CRE and clouds to increase in the tuning parameters  
17 from minimum to maximum values in Table 1.

18 The tuning parameters, which are especially effective in controlling the shortwave CRE, are  
19 *wcbmax* and *albice*; *wcbmax* and *albice* can change the SCRE by more than  $10 \text{ W/m}^2$  over  
20 low-latitude oceans and the Arctic, respectively (Figures 7a,j).

21 The parameter *wcbmax* is the maximum cumulus updraft velocity at the cloud base.  
22 Increasing the parameter leads to an increase in the cloud amount over low-latitude oceans  
23 (Figure A1a), which would increase the shortwave reflection by clouds and contribute to the  
24 negative increase in the SCRE, as indicated by the blue colour in Figure 7a. Indeed, the  
25 geographical distribution of the changes in the cloud amount and SCRE are similar to each  
26 other, which is consistent with the above-mentioned argument (Figures A1a, 7a).

27 *Albice* is the albedo of ice and snow. Increasing the parameter leads to an increase in the  
28 clear-sky albedo in high latitudes covered with ice and snow, which also decreases the albedo  
29 contrast between the clear- and all-sky components. Because the SCRE is proportional to this  
30 albedo contrast, it approaches zero by definition. Indeed, the SCRE shows a positive increase  
31 in high latitudes, as indicated by the red colour in Figure 7j, which is consistent with the  
32 above-mentioned argument. In addition, increasing the *albice* leads to the decrease in cloud



1 amount and cloud optical thickness in the Arctic (Figures A1j, A2j), which is also consistent  
2 with the change in SCRE (Figure 7j).

3 We confirmed in Figures 2a and 3e that the parametric uncertainty of the SCRE bias is  
4 exceptionally large in the Arctic compared with other latitudes. In the Arctic, albice is the  
5 most effective parameter controlling the SCRE based on Figure 7. We therefore surmise that  
6 the large uncertainty in the SCRE bias is mainly caused by perturbing the albice.

7 In addition to the wcbmax and albice, other parameters, such as clmd, vicec, b1, alp1, and  
8 ucmin, have a considerable impact on the SCRE (Figures 7c,d,e,g,i). Tuning these parameters  
9 leads to changes in the SCRE, which are consistent with the changes in the cloud amount or  
10 cloud optical thickness or in both of them (Figures A1, A2). To reduce the negative SCRE  
11 bias in low-latitude oceans, as shown in Figure 3a, the tuning of wcbmax, clmd, vicec, and b1  
12 would be effective. On the other hand, the impact of tuning precz0, faz1, and tnuw would be  
13 relatively small.

14 Focusing on the longwave CRE, we find that the most effective parameters are wcbmax and  
15 vicec; wcbmax and vicec can change the LCRE by more than  $10 \text{ W/m}^2$  in low latitudes  
16 (Figures 8a,d).

17 Increasing the wcbmax leads to changes in the cloud top pressure, which decreases in  
18 tropical Africa, western tropical Pacific, and the South Pacific Convergence Zone, while it  
19 increases in the subtropics, especially around South and Southeast Asia (Figure A3a). The  
20 decrease (increase) in the cloud top pressure would lead to a decrease (increase) in the cloud  
21 top temperature and upward longwave radiation, which would contribute to the increase  
22 (decrease) in the greenhouse effect of clouds and the LCRE. The geographical distribution of  
23 the changes in the cloud top pressure and LCRE are similar to each other, which is consistent  
24 with the above-mentioned argument (Figures A3a,8a).

25 The vicec parameter is a factor for the icefall speed. Increasing the parameter causes the  
26 increase in the icefall speed, decrease in the cloud amount (Figure A1d), and increase in the  
27 cloud top pressure (Figure A3d). Such changes of the cloud properties would contribute to the  
28 decrease of the greenhouse effect of clouds, which is consistent with the decrease in LCRE, as  
29 shown in Figure 8d.

30



## 1 6 Conclusions and Discussion

2 To discuss how much of the biases in the TOA radiation and clouds can be removed by  
3 parameter tuning in the present-day simulation with a climate model of the CMIP5 generation,  
4 we used a low-resolution version of the MIROC5 AOGCM and compared the output of the  
5 PPE experiment in the pre-industrial control setting with satellite observation data. We  
6 evaluated the biases in the TOA radiation and clouds and quantified the parametric  
7 uncertainty of the biases. We used the output of the PPE experiment without flux adjustment,  
8 which is consistent with the experimental design of the CMIP5. The results indicate that  
9 removing or changing the sign of the biases by parameter tuning only is difficult. Especially,  
10 the cooling bias of the SCRE in low latitudes could not be removed, neither in the zonal mean  
11 nor at each latitude–longitude grid point. The bias was related to the overestimation of both  
12 the cloud amount and cloud optical thickness, which could not be removed by parameter  
13 tuning either. However, they could be alleviated by tuning parameters such as the maximum  
14 cumulus updraft velocity at the cloud base. On the other hand, the bias of the SCRE in the  
15 Arctic was sensitive to parameter tuning. It could be removed by tuning parameters such as  
16 the albedo of ice and snow both in the zonal mean and at each grid point.

17 The results of the present study have implications for the future development of MIROC.  
18 Parameter tuning has only a limited capability of controlling the SCRE biases over low-  
19 latitude oceans and the Southern Ocean in MIROC5. Therefore, modifying the model  
20 structure should be given a high priority to effectively alleviate the biases. The results  
21 underline the importance of improving parameterizations based on cloud process studies. In  
22 MIROC5, the overestimation of the low-top cloud amount over low-latitude oceans is  
23 accompanied by the dry bias in the free troposphere above low-top clouds, suggesting that  
24 vertical mixing in the lower troposphere, such as that caused by shallow convection, is  
25 insufficient. On the other hand, the SCRE bias in the Arctic can be fully controlled by tuning  
26 the albedo of snow and ice in the current model structure. However, we expect that the albedo  
27 will be predicted or diagnosed with a more physically-based parameterization in the future  
28 rather than being specified as a tuning parameter, which would make the tuning of the SCRE  
29 more difficult.

30 The present study also has implications for the inter-model difference in the CRE simulated  
31 by the CMIP5 MME. The SCRE and LCRE simulated by the CMIP5 MME show a large  
32 inter-model spread. The spread is larger than that in MIROC5-PPE; therefore, the observation



1 data are within the range of the CMIP5 ensemble members for both the global mean and zonal  
2 mean values (Dolinar et al. 2015, Flato et al. 2013). This large spread in CMIP5 MME stems  
3 from the inter-model difference in both the model structure and specified parameter settings.  
4 The results of the present study indicate that specified parameter settings can explain only a  
5 small part of the inter-model spread in CMIP5 MME, suggesting that most of the spread is  
6 attributable to the difference in the model structure. This is consistent with the view that  
7 modifying the model structure is important to alleviate the biases in SCRE and LCRE.

8 However, we should note that the results of the model evaluation presented here depend on  
9 the design of the PPE experiment. For example, we restricted the number of the perturbed  
10 parameters to ten and that of the PPE members to 56 based on the amount of available  
11 computational resources. If we increased the number of the perturbed parameters and PPE  
12 members, the inter-model difference of the TOA radiation and cloud biases might be larger  
13 than that of the present study. The importance of the PPE design to obtain large inter-model  
14 spread is illustrated by Yamazaki et al. (2013) who conducted a PPE experiment with an  
15 AOGCM, HadCM3. They perturbed 33 parameters to create 20000 members in the PPE  
16 experiment. Although they subsampled the PPE members so that the TOA radiation balance is  
17 close to the observation, as was done by Shiogama et al. (2012), they showed that the inter-  
18 model difference of the climate sensitivity is larger than that of MIROC5-PPE or CMIP MME.

19 The choice of the model used for the PPE experiment is another important factor. If we  
20 employed a model other than MIROC5, the biases in the TOA radiation and clouds would be  
21 notably different from what we presented. Klein et al. (2013) reported that the bias of having  
22 too many optically thick clouds has been reduced from CFMIP1 to CFMIP2 MME, with the  
23 best models having eliminated this bias. If we used a model with a very small bias in optically  
24 thick clouds, we might be able to change the sign of the bias by parameter tuning only.  
25 Therefore, the dominance of structure-oriented bias as illustrated by the MIROC5-PPE does  
26 not necessarily indicate unimportance of the parameter-oriented bias in general, as the latter is  
27 a function of the former.

28 Another issue is whether we should include models with a large TOA radiation imbalance in  
29 the PPE members. We did not include such models because they are not used for future  
30 projections in the CMIP5 MME. However, such models could also be included in the PPE if  
31 we applied flux adjustment at the sea surface to suppress climate drift, which might increase  
32 the parametric uncertainty of the biases compared with the present study. For example,



1 Yamazaki et al. (2013) reported that the parametric uncertainty of the climate sensitivity  
2 increases by adopting models with a large TOA radiation imbalance in their PPE experiment  
3 using HadCM3 AOGCM. Collins et al. (2006) also conducted a PPE experiment using  
4 HadCM3 AOGCM with flux adjustment. They showed that the parametric uncertainty of the  
5 TOA shortwave radiation in the global and annual mean is  $\sim 20 \text{ W/m}^2$ , which is much larger  
6 than the results in the present study.

7 Whether the main conclusions in the present study are affected by the uncertainty in the PPE  
8 design is a subject of future studies. Based on a previous study, however, we speculate that  
9 removing the SCRE cooling bias over subtropical oceans by parameter tuning only might be  
10 difficult, even if we increased the PPE members by applying flux adjustment. Yokohata et al.  
11 (2012) evaluated the SCRE bias of PPE experiments under present climate conditions using  
12 an AOGCM and two ASGCMs with flux adjustment and an AGCM with prescribed SST.  
13 They reported that the cooling bias appears over subtropical oceans in almost all PPE  
14 members. This result is consistent with the idea that Suppressed Imbalance Sampling adopted  
15 in the present study is not the only reason for the robustness of the SCRE cooling bias, which  
16 cannot be removed by parameter tuning.

17 As discussed above, the obtained results of the PPE experiment are specific to the model and  
18 experimental design. Whether the results are applicable to other models or PPE experiments  
19 remains uncertain. However, the present study illustrates the benefit of PPE experiments,  
20 which provide useful information regarding the model development strategy, namely, the  
21 effectiveness and limitations of parameter tuning. Based on the results of the present study, a  
22 parameterization for shallow convection was implemented in MIROC6 to alleviate the cloud  
23 bias over low-latitude oceans. Conducting PPE experiments with the future versions of  
24 MIROC is advisable to update our knowledge on the parametric uncertainty, which depends  
25 on the model structure; PPE experiments without flux adjustment using AOGCMs other than  
26 MIROC5 would also be useful to evaluate the biases in the simulated present climates, which  
27 are relevant for future projections in the CMIP5 MME.

28

## 29 **7 Code and data availability**

30 Source code of MIROC5, associated with this study is available to those who conduct  
31 collaborative research with the model users under licence from copyright holders. For further  
32 information on how to obtain the code please contact the corresponding author. The data from



1 the model simulations and observations used in the analyses are available from the  
2 corresponding author upon request.

3

#### 4 **Appendix A: Impact of parameter tuning on ISCCP cloud properties**

5 The regression coefficients of the ISCCP cloud properties (cloud amount, cloud optical  
6 thickness, and cloud top pressure) on tuning parameters are shown here to help readers  
7 interpret the CRE changes in Figures 7 and 8.

8

#### 9 **Acknowledgements**

10 The authors thank Masahide Kimoto, Youichi Kamae, and Hideaki Kawai for continuing  
11 support and discussion. The authors also thank Editage ([www.editage.jp](http://www.editage.jp)) for English  
12 language editing. This work was supported by the Program for Risk Information on Climate  
13 Change (SOUSEI program) of the Ministry of Education, Culture, Sports, Science and  
14 Technology (MEXT), Japan. HS was supported by Grant-in-Aid 26281013 from the MEXT  
15 of Japan. The Earth Simulator at JAMSTEC and NEC SX at NIES were used to perform the  
16 model simulations.

17



## 1 **References**

- 2 Barkstrom, B. R. (1984) The Earth Radiation Budget Experiment (ERBE), *Bull. Amer.*  
3 *Meteor. Soc.*, 65, 1170-1185.
- 4 Bodas-Salcedo, A., M. J. Webb, S. Bony, H. Chepfer, J.-L. Dufresne, S. A. Klein, Y. Zhang,  
5 R. Marchand, J. M. Haynes, R. Pincus, and V. O. John (2011) COSP-satellite simulation  
6 software for model assessment, *Bulletin of the American Meteorological Society*, 1023-1043.
- 7 Bodas-Salcedo, A., K. D. Williams, M. A. Ringer, I. Beau, J. N. S. Cole, J.-L. Dufresne, T.  
8 Koshiro, B. Stevens, Z. Wang, and T. Yokohata (2014) Origins of the solar radiation biases  
9 over the Southern Ocean in CFMIP2 models, *J. Climate*, 27, 41-56.
- 10 Ceppi, P., Y.-T. Hwang, D. M. W. Frierson, and D. L. Hartmann (2012) Southern Hemisphere  
11 jet latitude biases in CMIP5 models linked to shortwave cloud forcing, *Geophys. Res. Lett.*,  
12 39, L19708, doi:10.1029/2012GL053115.
- 13 Chepfer, H., S. Bony, D. Winker, M. Chiriaco, J.-L. Dufresne, and G. Seze (2008) Use of  
14 CALIPSO lidar observations to evaluate the cloudiness simulated by a climate model,  
15 *Geophys. Res. Lett.*, 35, L15704, doi:10.1029/2008GL034207.
- 16 Chepfer, H., S. Bony, D. Winker, G. Cesana, J.-L. Dufresne, P. Minnis, C. J. Stubenrauch,  
17 and S. Zeng (2010) The GCM-oriented CALIPSO cloud product (CALIPSO-GOCCP), *J.*  
18 *Geophys. Res.*, 115, D00H16.
- 19 Chikira, M., and M. Sugiyama (2010) A cumulus parameterization with state-dependent  
20 entrainment rate. Part 1: description and sensitivity to temperature and humidity profiles, *J.*  
21 *Atmos. Sci.*, 67, 2171-2193.
- 22 Collins, M., B. B. Booth, G. R. Harris, J. M. Murphy, D. M. H. Sexton, and M. J. Webb  
23 (2006) Towards quantifying uncertainty in transient climate change, *Clim. Dyn.*, 27, 127-147.
- 24 Dolinar, E. K., X. Dong, B. Xi, J. H. Jiang, and H. Su (2015) Evaluation of CMIP5 simulated  
25 clouds and TOA radiation budgets using NASA satellite observations, *Clim. Dyn.*, 44, 2229-  
26 2247, doi:10.1007/s00382-014-2158-9.
- 27 Flato, G., J. Marotzke, B. Abiodun, P. Braconnot, S.C. Chou, W. Collins, P. Cox, F. Driouech,  
28 S. Emori, V. Eyring, C. Forest, P. Gleckler, E. Guilyardi, C. Jakob, V. Kattsov, C. Reason,  
29 and M. Rummukainen (2013) Evaluation of Climate Models. In: *Climate Change 2013: The*  
30 *Physical Science Basis. Contribution of Working Group I to the Fifth Assessment Report of*



- 1 the Intergovernmental Panel on Climate Change [Stocker, T.F., D. Qin, G.-K. Plattner, M.  
2 Tignor, S.K. Allen, J. Boschung, A. Nauels, Y. Xia, V. Bex and P.M. Midgley (eds.)].  
3 Cambridge University Press, Cambridge, United Kingdom and New York, NY, USA.
- 4 Jackson, L. C., M. Vellinga, and G. R. Harris (2012) The sensitivity of the meridional  
5 overturning circulation to modelling uncertainty in a perturbed physics ensemble without flux  
6 adjustment, *Clim. Dyn.*, 39, 277-285.
- 7 Klein, S. A. and C. Jakob (1999) Validation and sensitivities of frontal clouds simulated by  
8 the ECMWF model, *Mon. Wea. Rev.*, 127, 2514-2531.
- 9 Klein, S. A., Y. Zhang, M. D. Zelinka, R. Pincus, J. Boyle, and P. J. Gleckler (2013) Are  
10 climate model simulations of clouds improving? An evaluation using the ISCCP simulator, *J.*  
11 *Geophys. Res.*, 118, 1329-1342.
- 12 Loeb, N. G., B. A. Wielicki, D. R. Doelling, G. L. Smith, D. F. Keyes, S. Kato, N. Manalo-  
13 Smith, and T. Wong (2009) Toward optimal closure of the Earth's top-of-atmosphere  
14 radiation budget, *J. Climate*, 22, 748-766.
- 15 Murphy, J. M., D. M. H. Sexton, D. N. Barnett, G. S. Jones, M. J. Webb, M. Collins, and D.  
16 A. Stainforth (2004) Quantification of modelling uncertainties in a large ensemble of climate  
17 change simulations, *Nature*, 430, 768-772.
- 18 Nakanishi, M., and H. Niino (2004) An improved Mellor-Yamada level-3 model with  
19 condensation physics: its design and verification, *Boundary-Layer Meteorol.*, 112, 1-31.
- 20 Nam, C., S. Bony, J.-L. Dufresne, and H. Chepfer (2012) The 'too few, too bright' tropical  
21 low-cloud problem in CMIP5 models, *Geophys. Res. Lett.*, 39, L21801.
- 22 Pincus, R., S. Platnick, S. A. Ackerman, R. S. Hemler, and R. J. P. Hofmann (2012)  
23 Reconciling simulated and observed views of clouds: MODIS, ISCCP, and the limits of  
24 instrument simulators, *J. Climate* 25, 4699-4720.
- 25 Rossow, W. B., A. W. Walker, D. Beuschel, and M. Roiter (1996) International Satellite  
26 Cloud Climatology Project (ISCCP) documentation of new cloud datasets. WMO/TD 737,  
27 World Climate Research Programme (ICSU and WMO), 115pp.
- 28 Shiogama, H., M. Watanabe, M. Yoshimori, T. Yokohata, T. Ogura, J. D. Annan, J. C.  
29 Hargreaves, M. Abe, Y. Kamae, R. O'ishi, R. Nobui, S. Emori, T. Nozawa, A. Abe-Ouchi,  
30 and M. Kimoto (2012) Perturbed physics ensemble using the MIROC5 coupled atmosphere-



- 1 ocean GCM without flux corrections: experimental design and results, *Clim. Dynam.*,  
2 doi:10.1007/s00382-012-1441-x.
- 3 Takata, K., S. Emori, and T. Watanabe (2003) Development of the minimal advanced  
4 treatments of surface interaction and runoff, *Global Planet. Change*, 38, 209-222.
- 5 Takemura, T., T. Nozawa, S. Emori, T. Y. Nakajima, and T. Nakajima (2005) Simulation of  
6 climate response to aerosol direct and indirect effects with aerosol transport-radiation model,  
7 *J. Geophys. Res.*, 110, D02202, doi:10.1029/2004JD005029.
- 8 Takemura, T., M. Egashira, K. Matsuzawa, H. Ichijo, R. O'ishi, and A. Abe-Ouchi (2009) A  
9 simulation of the global distribution and radiative forcing of soil dust aerosols at the Last  
10 Glacial Maximum, *Atmos. Chem. Phys.*, 9, 3061-3073.
- 11 Trenberth, K. E. and J. T. Fasullo (2010) Simulation of present-day and twenty-first-century  
12 energy budgets of the southern oceans, *J. Climate*, 23, 440-454.
- 13 Watanabe, M., T. Suzuki, R. O'ishi, Y. Komuro, S. Watanabe, S. Emori, T. Takemura, M.  
14 Chikira, T. Ogura, M. Sekiguchi, K. Takata, D. Yamazaki, T. Yokohata, T. Nozawa, H.  
15 Hasumi, H. Tatebe, and M. Kimoto (2010) Improved climate simulation by MIROC5: mean  
16 states, variability, and climate sensitivity, *J. Climate*, 23, 6312-6335.
- 17 Webb, M., C. Senior, S. Bony, and J. J. Morcrette (2001) Combining ERBE and ISCCP data  
18 to assess clouds in the Hadley Centre, ECMWF and LMD atmospheric climate models, *Clim.*  
19 *Dynam.*, 17, 905-922.
- 20 Wielicki, B. A., B. R. Barkstrom, E. F. Harrison, R. B. Lee III, G. L. Smith, and J. E. Cooper  
21 (1996) Clouds and the Earth's Radiant Energy System (CERES): An Earth observing system  
22 experiment, *Bull. Amer. Meteorol. Soc.*, 77, 5, 853-868.
- 23 Wilson, D. R., and S. P. Ballard (1999) A microphysically based precipitation scheme for the  
24 UK Meteorological Office Unified Model, *Q. J. R. Meteorol. Soc.*, 125, 1607-1636.
- 25 Yamazaki, K., D. J. Rowlands, T. Aina, A. T. Blaker, A. Bowery, N. Massey, J. Miller, C.  
26 Rye, S. F. B. Tett, D. Williamson, Y. H. Yamazaki, and M. R. Allen (2013) Obtaining diverse  
27 behaviors in a climate model without the use of flux adjustments, *J. Geophys. Res.*, 118, 1-13.
- 28 Yokohata, T., J. D. Annan, M. Collins, C. S. Jackson, M. Tobis, M. J. Webb, and J. C.  
29 Hargreaves (2012) Reliability of multi-model and structurally different single-model  
30 ensembles, *Clim. Dynam.*, 39, 599-616.



- 1 Zelinka, M. D., S. A. Klein, and D. L. Hartmann (2012) Computing and partitioning cloud  
2 feedbacks using cloud property histograms. Part 1: Cloud radiative kernels, *J. Climate*, 25,  
3 3715-3735.
- 4 Zhang, M. H., W. Y. Lin, S. A. Klein, J. T. Bacmeister, S. Bony, R. T. Cederwall, A. D. Del  
5 Genio, J. J. Hack, N. G. Loeb, U. Lohmann, P. Minnis, I. Musat, R. Pincus, P. Stier, M. J.  
6 Suarez, M. J. Webb, J. B. Wu, S. C. Xie, M. -S. Yao, and J. H. Zhang (2005) Comparing  
7 clouds and their seasonal variations in 10 atmospheric general circulation models with  
8 satellite measurements, *J. Geophys. Res.*, 110, D15S02.
- 9 Zhang, Y., S. Xie, C. Covey, D. D. Lucas, P. Gleckler, S. A. Klein, J. Tannahill, C. Doutriaux,  
10 and R. Klein (2012) Regional assessment of the parameter-dependent performance of CAM4  
11 in simulating tropical clouds, *Geophys. Res. Lett.*, 39, L14708.
- 12 Zhang, Y., W. B. Rossow, A. A. Lacis, V. Oinas, and M. I. Mishchenko (2004) Calculation of  
13 radiative fluxes from the surface to top of atmosphere based on ISCCP and other global data  
14 sets: Refinements of the radiative transfer model and the input data, *J. Geophys. Res.*, 109,  
15 D19105, doi:10.1029/2003JD004457.
- 16



1 Table 1. List of physics parameters that were varied in the MIROC5-PPE.

Name	Category	Description	Standard	Min	Max
wcbmax <sup>a</sup>	Cumulus	Maximum cumulus updraft velocity at cloud base (m/s)	1.7	0.7	2.8
precz0 <sup>a</sup>	Cumulus	Base height for cumulus precipitation (m)	500	200	1000
clmd <sup>a</sup>	Cumulus	Entrainment efficiency (ND)	0.51	0.4	0.6
vicec <sup>b</sup>	Cloud	Factor for ice falling speed (m <sup>0.474</sup> /s)	38	25	40
b1 <sup>c</sup>	Cloud	Berry parameter (m <sup>3</sup> /kg)	0.09	0.07	0.11
faz1 <sup>d</sup>	Turbulence	Factor for PBL overshooting (ND)	1.5	1	3
alp1 <sup>d</sup>	Turbulence	Factor for length scale L <sub>T</sub> (ND)	0.23	0.16	0.3
tnuw <sup>c</sup>	Aerosol	Timescale for nucleation (s)	18000	14400	21600
ucmin <sup>c</sup>	Aerosol	Minimum cloud droplet number (liquid) (m <sup>-3</sup> )	2.5×10 <sup>7</sup>	2.2×10 <sup>7</sup>	3.0×10 <sup>7</sup>
alb <sup>e</sup>	Surface	Albedo of ice and snow <sup>f</sup>	Medium	Low	High

2 <sup>a</sup> Chikira and Sugiyama (2010)

3 <sup>b</sup> Wilson and Ballard (1999)

4 <sup>c</sup> Takemura et al. (2005, 2009)

5 <sup>d</sup> Nakanishi and Niino (2004)

6 <sup>e</sup> Takata et al. (2003) and Watanabe et al. (2010)

7 <sup>f</sup> “alb” indicates a collection of eight parameters corresponding to the albedo of ice and snow over sea and land

8

9 Table 2. Observation data used for the model evaluation. All data are monthly means.

Variable	Dataset	Period	References
Top-of-atmosphere radiative fluxes	CERES-EBAF	March 2000–October 2005	Loeb et al. (2009)
	ERBE-S9	January 1985–December 1989	Barkstrom (1984)
	ISCCP-FD	January 1986–December 1990	Zhang et al. (2004)
Cloud fraction	GCM simulator-oriented ISCCP cloud product	July 1983–June 2008	Pincus et al. (2012), Rossow et al. (1996)
	CALIPSO-GOCCP	June 2006–December 2010	Chepfer et al. (2010)

10

11

12

13



1  
2  
3  
4  
5  
6  
7  
8  
9  
10  
11  
12  
13  
14  
15  
16  
17  
18  
19  
20  
21  
22  
23  
24  
25  
26

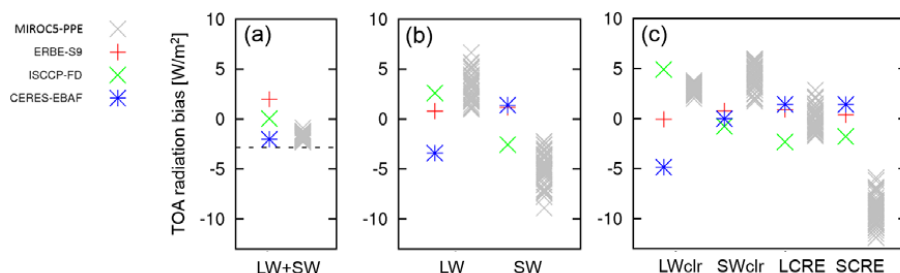


Figure 1.

TOA radiation bias in the global annual mean for (a) net, (b) longwave and shortwave, (c) longwave clear-sky, shortwave clear-sky, longwave CRE, and shortwave CRE components. The biases are with respect to the average of three observational data, namely, ERBE-S9, ISCCP-FD, and CERES-EBAF. The net radiation of zero with no TOA imbalance is indicated by the dashed line in (a). The unit is  $W/m^2$  and the signs are positive downward.



1  
2  
3  
4  
5  
6  
7  
8  
9  
10  
11  
12  
13  
14  
15  
16  
17  
18  
19  
20  
21  
22  
23  
24  
25  
26

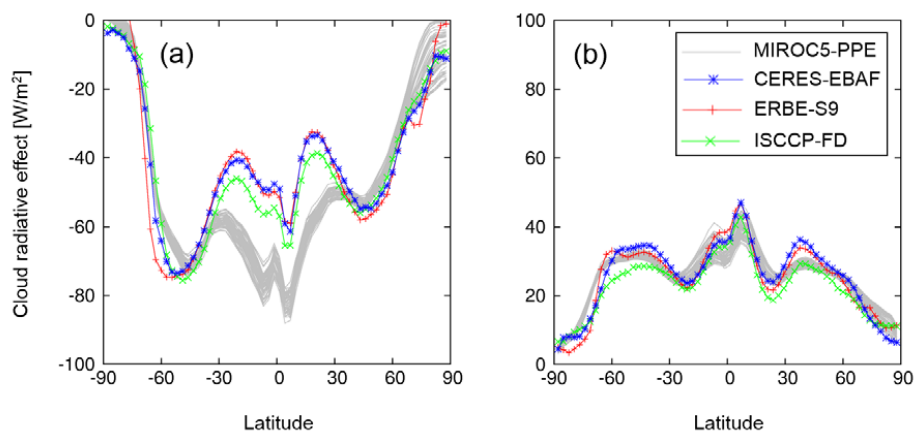


Figure 2.

TOA radiation in the zonal annual mean for the (a) shortwave CRE and (b) longwave CRE components. The unit is  $\text{W/m}^2$  and the signs are positive downward.



1  
2  
3  
4  
5  
6  
7  
8  
9  
10  
11  
12  
13  
14  
15  
16  
17  
18  
19  
20  
21  
22  
23  
24  
25  
26

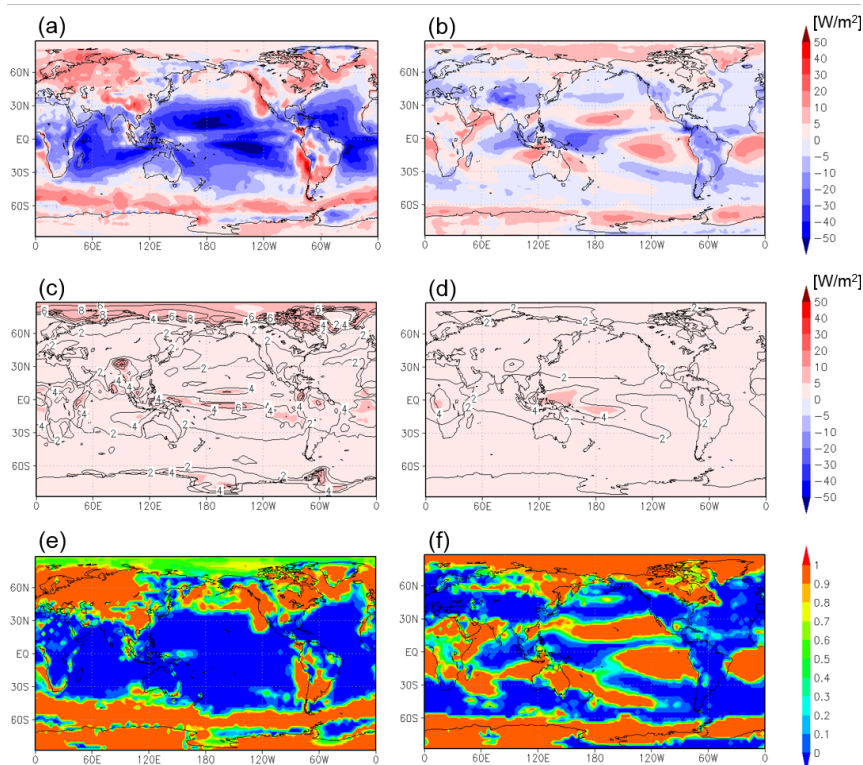


Figure 3.

TOA radiation bias in the annual mean for the (a) shortwave CRE and (b) longwave CRE components. The biases are for the ensemble mean of MIROC5-PPE with respect to CERES-EBAF. Standard deviation of the TOA radiation bias among the PPE ensemble members for the (c) shortwave CRE and (d) longwave CRE. Fraction of the PPE ensemble members, which have positive signs of the TOA radiation bias, for the (e) shortwave CRE and (f) longwave CRE.



1

2

3

4

5

6

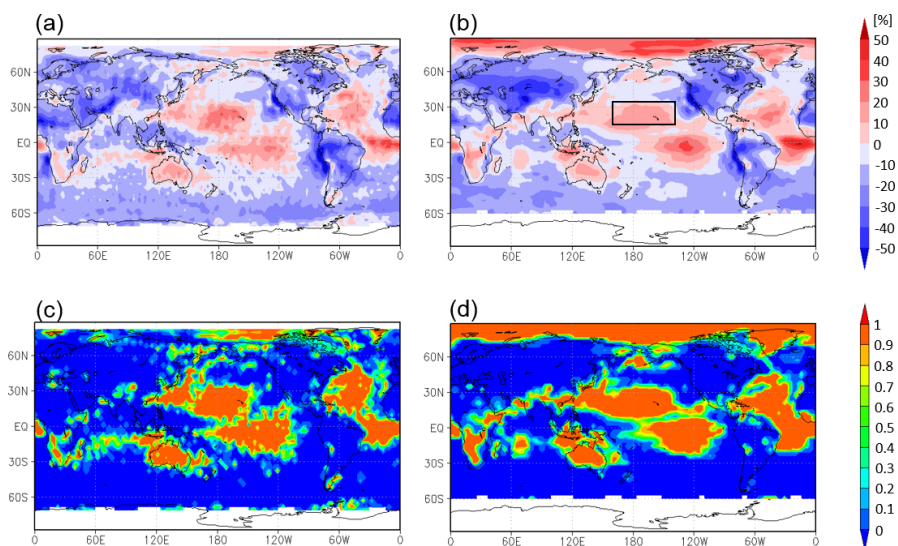
7

8

9

10

11



12

Figure 4.

13

Cloud amount bias in the July mean with respect to the (a) CALIPSO and (b) ISCCP

14

observations. The biases are for the ensemble mean of MIROC5-PPE. Fraction of the

15

PPE ensemble members, which have positive signs of the cloud amount bias, with

16

respect to (c) CALIPSO and (d) ISCCP observation.

17

18

19

20

21

22

23

24

25



1  
2  
3  
4  
5  
6  
7  
8  
9  
10  
11  
12  
13  
14  
15  
16  
17  
18  
19  
20  
21  
22  
23  
24  
25  
26

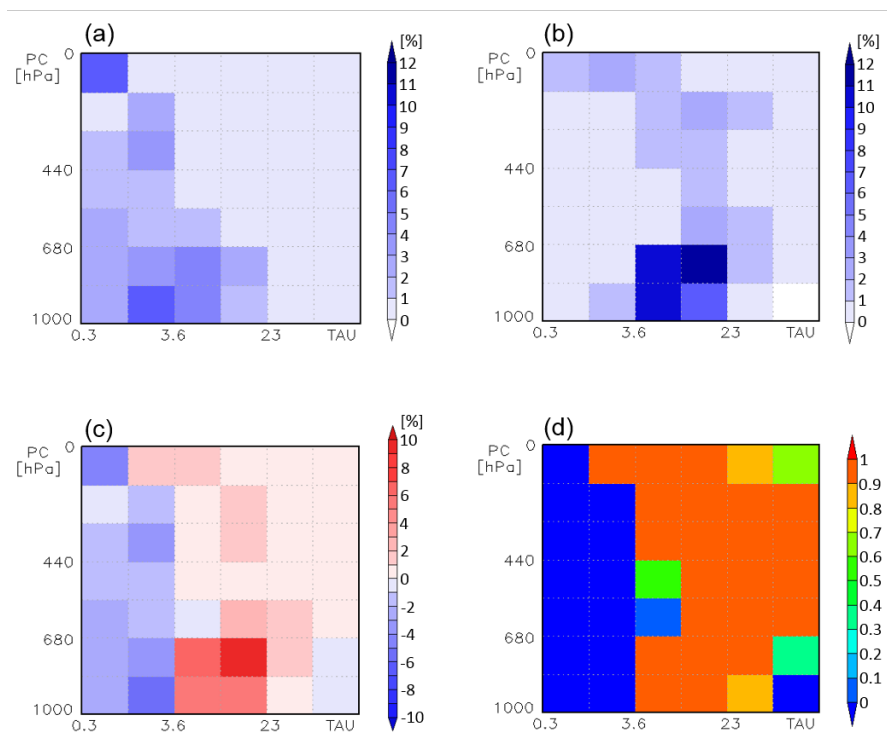


Figure 5.

IISCCP cloud amount of the July mean for the Hawaiian Trade Cumulus Region (15–35N, 160E–140W), indicated by the black square in Figure 4b, for different categories of the cloud top pressure (PC) and cloud optical thickness (TAU). Each panel is for (a) IISCCP observation, (b) MIROC5-PPE ensemble mean, (c) model bias, namely (b) minus (a), and (d) fraction of the PPE ensemble members with positive bias.



1  
2  
3  
4  
5  
6  
7  
8  
9  
10  
11  
12  
13  
14  
15  
16  
17  
18  
19  
20  
21  
22  
23  
24  
25  
26

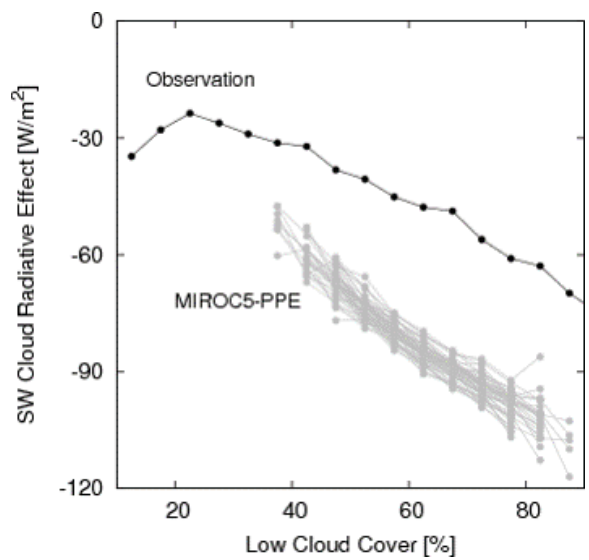


Figure 6.  
Relationship between the non-overlapped low cloud amount and shortwave CRE of the July mean for the Hawaiian Trade Cumulus Region.



1  
2  
3  
4  
5  
6  
7  
8  
9  
10  
11  
12  
13  
14  
15  
16  
17  
18  
19  
20  
21  
22  
23  
24  
25  
26

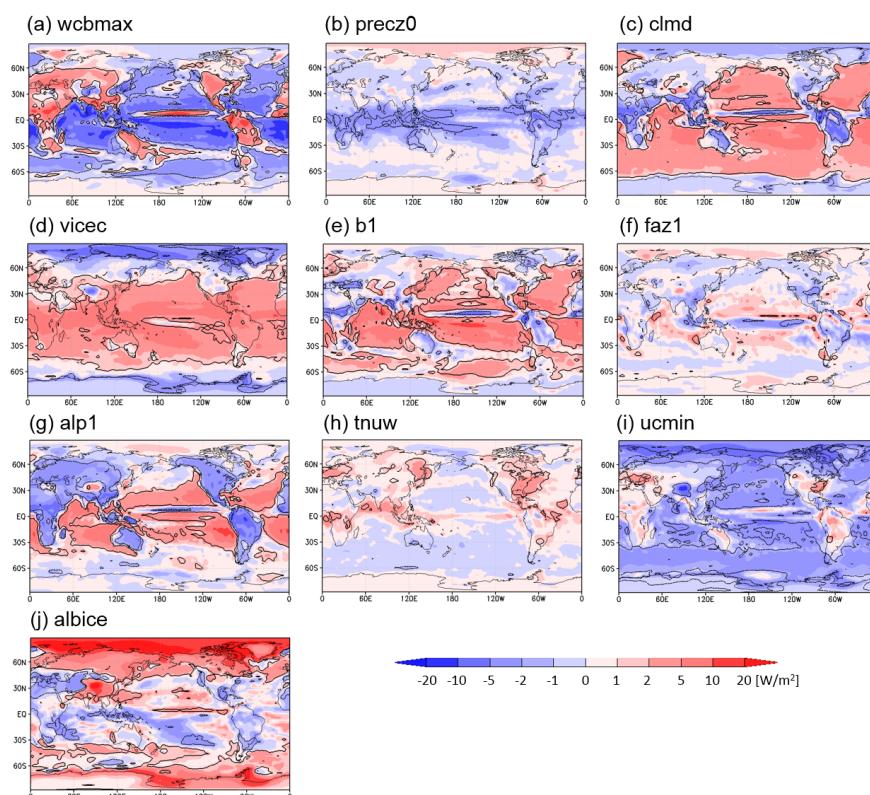


Figure 7.

Regression coefficient of the annual mean TOA shortwave CRE on the tuning parameters calculated with the 56 samples of the MIROC5-PPE. The definition of the tuning parameters is shown in Table 1. The tuning parameters are normalized to the range of [0,1]. The black curves indicate the threshold of the statistical significance with 5% level.



1  
2  
3  
4  
5  
6  
7  
8  
9  
10  
11  
12  
13  
14  
15  
16  
17  
18  
19  
20  
21  
22  
23  
24  
25  
26

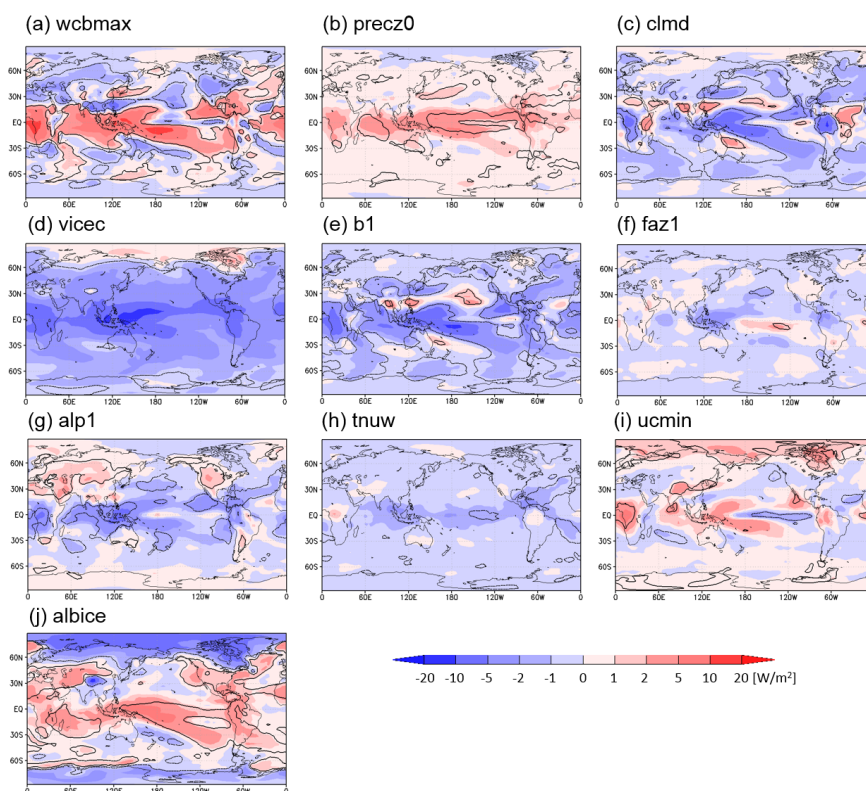


Figure 8.

Regression coefficient of the annual mean TOA longwave CRE on the tuning parameters calculated using the 56 samples of the MIROC5-PPE. The definition of the tuning parameters is shown in Table 1. The tuning parameters are normalized to the range of [0,1]. The black curves indicate the threshold of the statistical significance with 5% level.



1  
2  
3  
4  
5  
6  
7  
8  
9  
10  
11  
12  
13  
14  
15  
16  
17  
18  
19  
20  
21  
22  
23  
24  
25  
26

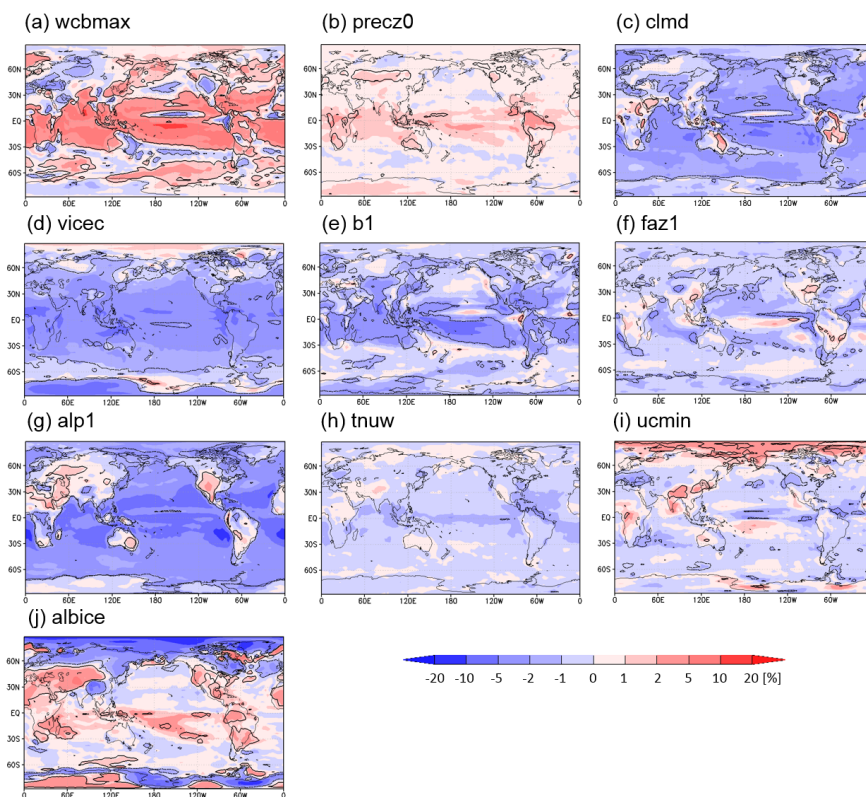


Figure A1.

Regression coefficient of the annual mean ISCCP cloud amount on the tuning parameters calculated using the 56 samples of the MIROC5-PPE. The definition of the tuning parameters is shown in Table 1. The tuning parameters are normalized to the range of [0,1]. The black curves indicate the threshold of the statistical significance with 5% level.



1  
2  
3  
4  
5  
6  
7  
8  
9  
10  
11  
12  
13  
14  
15  
16  
17  
18  
19  
20  
21  
22  
23  
24  
25  
26

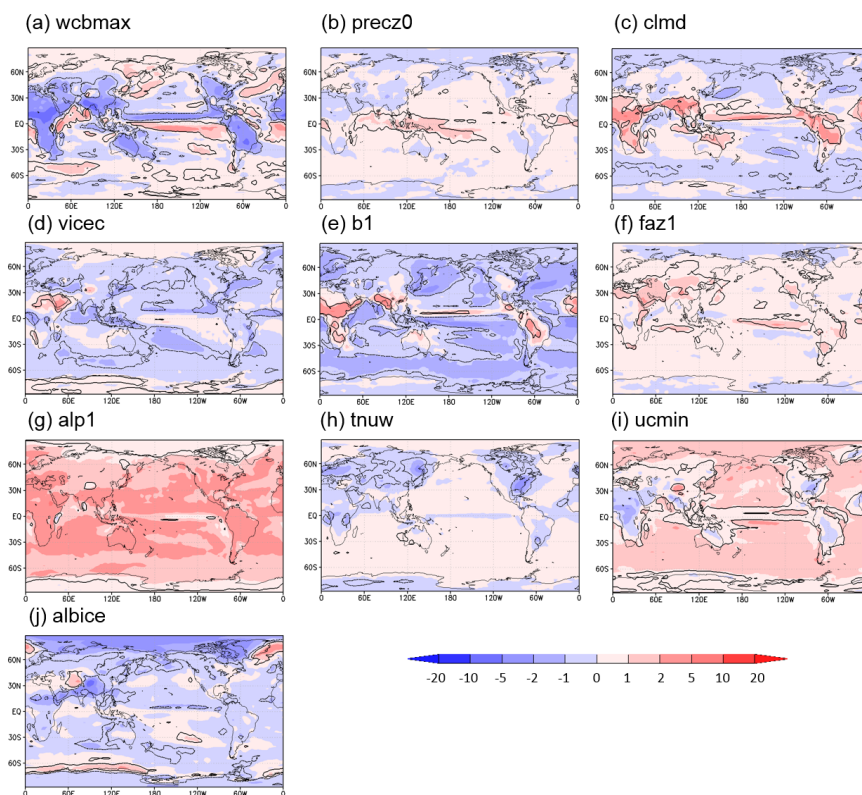


Figure A2.

Regression coefficient of the annual mean ISCCP cloud optical thickness on the tuning parameters calculated using the 56 samples of the MIROC5-PPE. The definition of the tuning parameters is shown in Table 1. The tuning parameters are normalized to the range of [0,1]. The black curves indicate the threshold of the statistical significance with 5% level.



1  
2  
3  
4  
5  
6  
7  
8  
9  
10  
11  
12  
13  
14  
15  
16  
17  
18  
19  
20  
21  
22  
23  
24

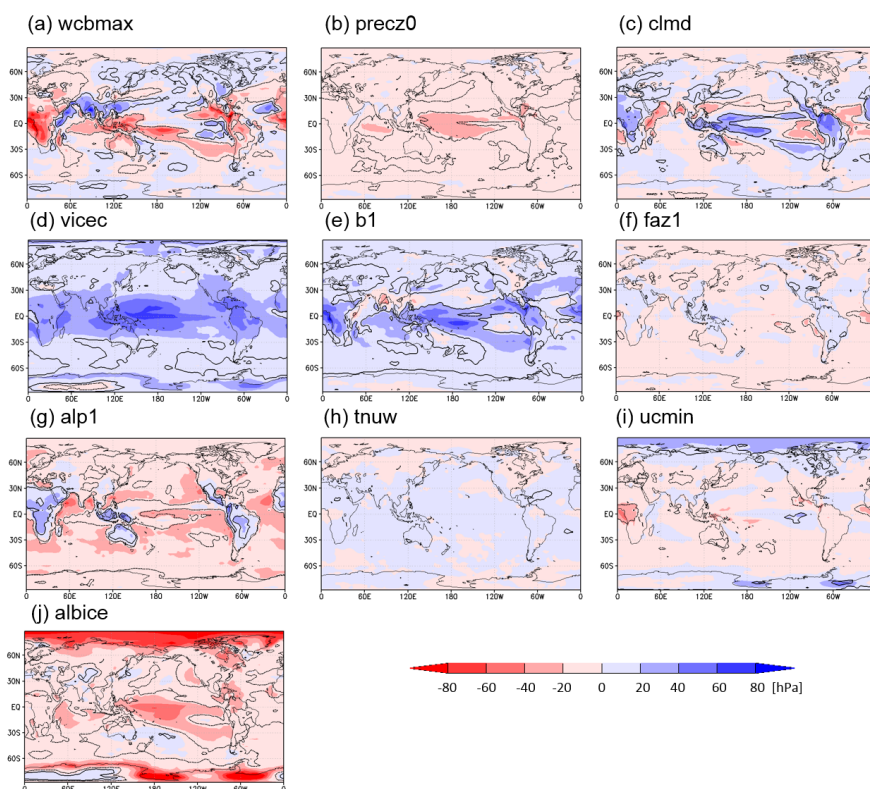


Figure A3.

Regression coefficient of the annual mean ISCCP cloud top pressure on the tuning parameters calculated using the 56 samples of the MIROC5-PPE. The definition of the tuning parameters is shown in Table 1. The tuning parameters are normalized to the range of [0,1]. The black curves indicate the threshold of the statistical significance with 5% level.